Synthesis, Characterization and DNA Interactions of $[Pt_3(TPymT)Cl_3]$, the Trinuclear Platinum(II) Complex of the TPymT ligand

Tiziano Marzo [a,b#], Damiano Cirri[b#], Lorenzo Ciofi[b], Chiara Gabbiani[a], Alessandro Feis[c], Nancy Di Pasquale[a], Matteo Stefanini[d], Tarita Biver[a*] and Luigi Messori[b*]

[a] Department of Chemistry and Industrial Chemistry (DCCI), University of Pisa, Via Moruzzi, 13, 56124 Pisa, Italy
[b] Laboratory of Metals in Medicine (MetMed), Department of Chemistry "U. Schiff", University of Florence, Via della Lastruccia 3, 50019 Sesto Fiorentino, Italy
[c] Department of Chemistry "U. Schiff", University of Florence, Via della Lastruccia 3, 50019 Sesto Fiorentino, Italy
[d] DI.V.A.L Toscana S.R.L., Via Madonna del Piano, 6, 50019 Sesto Fiorentino, Italy
#These two authors equally contributed

***Corresponding authors: (L. Messori) luigi.messori@unifi.it; +39 0554573388; (T. Biver) tarita.biver@unipi.it; +39 050 2219259**

Keywords: TPymT, Platinum, DNA, Anticancer drug, Coordination chemistry

ABSTRACT

The triplatinum complex of the 2,4,6-Tris(2-pyrimidyl)-1,3,5-triazine ligand, Pt_3TPymT hereafter, has been prepared and characterized for the first time. NMR studies point out that the three platinum(II) centers possess an identical coordination environment. The interactions of Pt_3TPymT with DNA were explored in comparison to the free ligand. Specifically, fluorescence, mass spectrometry, viscometry and melting measurements were carried out. In contrast to expectations, the obtained data reveal that no intercalative binding takes place; we propose that binding of Pt_3TPymT to DNA mainly occurs through external/groove binding.

1. INTRODUCTION

The 2,4,6-Tris(2-pyrimidyl)-1,3,5-triazine ligand (TPymT) has been known for more than 60 years [1] and still appears to be very attractive for its peculiar coordination chemistry properties. Indeed, this ligand has the potential to bind tightly three metal ions at three identical sites through a N3 donor set (Figure 1). However, only a limited number

of studies utilizing this ligand have appeared so far owing to its general unavailability, poor solubility in common solvents, and to the facile hydrolysis of the central triazine fragment; among these, the complexes of TPymT with Pb^{2+}, Tl^{+} and UO_2^{2+} were obtained and characterized by Lippard and co-workers several years ago [2]. The state of art of the coordination chemistry studies centred on this ligand has been recently recapitulated by Murugesu and coworkers [3]. In this frame, of particular interest are the recent results concerning the trisilver complex of TPymT, Ag_3TPymT, that was prepared and characterized by Murugesu et al [4]; notably, high resolution crystallographic results revealed the presence of an extended planar system.

We noticed that the platinum(II) complex of the TPymT ligand has not been reported and described so far, either in solution or in the solid state. We argued that this complex might be prepared and characterized quite straightforwardly in analogy to the case of the trisilver complex. In principle, the triplatinum complex of the TPymT ligand should exhibit a widely extended planar structure together with a highly cationic character and thus behave as an efficient intercalating agent for double helix DNA. If this is proved, this complex might be a good candidate for medicinal chemistry studies as a potential anticancer drug.

It is worthy reminding that platinum(II) complexes of thio-pyridyl-triazine are potential antitumor agents, with a cytotoxic activity greater than cisplatin and the free ligand [5]. Notably, ruthenium(II) diamino-triazine aquo-complexes were shown to strongly interact with DNA [6]. However, as for the possible use of this family of complexes as antitumor agents, to be best of our knowledge, only a Ru(II) complex has been tested [7]. In view of these arguments, we report here the synthesis and detailed chemical characterization of the triplatinum complex of TPymT and explore its interactions with various DNA molecules.

< Figure 1 near here>

2. MATERIALS AND METHODS

2.1 Double and single stranded DNA

Appropriate amounts of the ligand tris-2,4,6-(2-pyrimidyl)-1,3,5-triazine (TPymT, L) or of its platinum complex ($[(TPymT)Pt_3(Cl)_3]^{3+}$, Pt_3L^{3+}) were accurately weighted out and dissolved in the buffer or in dimethyl sulfoxide (DMSO), respectively. The stock solutions so obtained were ca. 10^{-3} M. The buffer is an aqueous solution of 0.1 M NaCl and 0.01 NaCac (sodium cacodylate) at pH 7.0. The water used always comes from an ultra-pure grade purification system (AriumPro, Sartorius). The molar concentration of either ligand or complex (i.e. dye, drug) will be indicated as C_D.

DNA was from calf thymus, and in particular a double helix B-form, highly polymerised salt from Sigma. It was sonicated to reduce its length to ca. 500 base pairs following a known procedure [8]. The molar concentration (in base pairs) of the DNA solutions, C_{DNA}, was spectrophotometrically evaluated (ε = 13200 M^{-1} cm^{-1} at λ = 260 nm, [NaCl] = 0.1 M, [NaCac] = 0.01 M, pH 7.0 [9]) The solutions of ethidium bromide solution (EB, purity > 99%, Sigma) were obtained by dissolving the appropriate amount of the solid in the buffer; their molar concentration (C_{EB}) was evaluated spectrophotometrically (ε = 5600 M^{-1} cm^{-1} at λ = 480 nm, [NaCl] = 0.1 M, [NaCac] = 0.01 M [10]).

The dodecameric oligonucleotide CTACGGTTTCAC (ODN) was purchased from Sigma-Aldrich and used without further purification and its ultra-pure water 10^{-3} M stock solution was stored at -20 °C. Solutions of ODN (10^{-5} M in ultra-pure water) were incubated for 72 h at 37° C at different complex:ODN ratios, i.e. 0.2:1 and 0.5:1 in the presence of 1% dimethylformamide (DMF).

2.2 Spectrophotometric analysis

Spectrophotometric measurements/titrations were done in triplicates on a double beam Shimadzu 2450 apparatus. Light emission measurements were done using a Perkin Elmer LS55 instrument. Both spectrophotometer and spectrofluorometer are thermostatted by a water bath (± 0.1 °C). The actual temperature inside the cell compartment was controlled

by a mini-thermometer. Any addition during spectroscopic titrations was done directly into the cell by means of a glass syringe connected to a micrometric screw (Mitutoyo, additions as small as 0.164 µL possible with high accuracy). In the case of the DNA melting experiments, care was taken to increase the temperature very slowly, so to ensure system stabilization before data reading (5°C/15' + 30' equilibration).

2.3 Viscosimetry

Viscosimetric experiments were carried out using a semi-micro Ubbelohde capillary (1.0 mL volume), immersed in a temperature-controlled water bath (± 0.1° C). Flow times were measured by a stop watch at least in quintuplicates.

2.4 Mass spectrometry

The electrospray mass spectrometric study (ESI-MS) of the oligonucleotide (ODN)-Pt_3L^{3+} mixture was performed by direct infusion at 10 µl min^{-1} flow rate in an TripleTOF® 5600+ System mass spectrometer (Sciex, Framingham, MA, U.S.A.), equipped with a TurboIonSpray® interface operating with an ESI probe. The MS source parameters were optimized and were as follows: negative polarity, Ionspray Voltage Floating (ISVF) -4500 V, Temperature (TEM) 400° C, Ion source Gas 1 (GS1) 40; Ion source Gas 2 (GS2) 30; Curtain Gas (CUR) 25, Declustering Potential (DP) -50 V, Collision Energy (CE) -10 V. For acquisition, Analyst TF software 1.7.1 (Sciex) was used and deconvoluted spectra were obtained by using the Bio Tool Kit version 2.2 tool for Peakview 2.2 software (Sciex). The mass spectrometer was operated with a resolving power greater than $30\,000_{fwhm}$ for TOF MS scans.

2.5 NMR Spectroscopy

NMR spectra were recorded at room temperature (25 ± 1° C) in a Bruker Avance III 400 spectrometer equipped with a Bruker Ultrashield 400 Plus superconducting magnet (resonating frequencies: 400.13, 100.61 MHz for ^{1}H, ^{13}C respectively) and a 5 mm PABBO BB-1H/D Z-GRD Z108618/0049 probe.

2.6 Raman spectroscopy

Raman spectra were measured with a Bruker MultiRAM FT-Raman spectrometer, equipped with a Nd:YAG laser emitting at 1064 nm. The spectral resolution was 4 cm^{-1}.

2.7 Cellular studies (WST-1)

Cells were seeded in a 96-well flat-bottomed plate (Corning-Costar, Corning, NY, USA); 2×10^{4} per well, 100 μL medium per well. Experiments were carried out in the range 10-150 μM (all experiments were performed in triplicate). After 24 h the medium was removed and replaced with fresh one containing the investigated compound at different concentrations. After further 24 h the medium was removed and wells added with medium containing 10 μL of WST-1 proliferation reagent. After 2 h of incubation, absorbance (proportional to the number of cells) was read at 450 nm to determine cells viability.

3. RESULTS AND DISCUSSION

3.1 Synthesis and characterisation of tris-2,4,6-(2-pyrimidyl)-1,3,5-triazine (TpymT) and $[Pt_3(TPymT)(Cl)_3]^{3+}\cdot 3OH^-$

Tris-2,4,6-(2-pyrimidyl)-1,3,5-triazine (TpymT) was synthetized modifying the procedure previously reported [11]. NH_4Br (65 mg, 0.66 mmol) and diisopropylethylamine (DIPEA, 113 µl, 0.66 mmol) were added to a suspension of 2-cyanopyrimidine (1.382 g, 13.2 mmol) in 1-pentanol (5 mL). The suspension was heated under stirring for 18 h in an oil bath kept at 135 °C. The reaction mixture was filtered and the solid extensively washed with acetonitrile. After washing, the pure product was obtained as a light brown solid in 73.5 % yield (1.015 g).

The product was identified by comparing its ^{1}HNMR spectrum [(DMSO-d_6, 400.13 MHz, 298K): 9.16 (d, 6H, J = 4.80 Hz); 7.82 (t, 3H, J = 4.84 Hz)] with the data reported in the literature [12] and further confirmation was obtained by recording ^{1}HNMR spectra of starting material (i.e. 2-pyrimidinecarbonitrile) and obtained product (i.e. TpymT) in D_2O (see Supplementary Information).

The trinuclear Pt^{2+} complex was prepared adding 140 mg (0.34 mmol) of K_2PtCl_4 to a suspension of 30 mg (0.097 mmol) of TPymT in ethanol (6 mL). The mixture was refluxed under stirring for 2 h; then, the solid precipitate was recovered in a Hirsch filter, washed with ultra-pure water and diethyl ether and dried under reduced pressure. The dark-brown product (78.1 mg; yield 85.9 %) was firstly characterized by elemental analysis for $C_{15}H_{12}Cl_3N_9O_3Pt_3$ [calculated C: 17.03%, H: 1.14%, N: 11.92%; experimental: C: 16.97%, H: 1.11%, N: 11.63%], then with ^{1}H and ^{13}C NMR experiments performed in D_2O and DMF-d_7. ^{1}HNMR (400.13MHz; DMF-d7): 9.43 (2H; d; J = 5.28 Hz); 8.10 (^{1}H; t; J = 5.28 Hz) (Figure 2), ^{13}CNMR (100.61MHz; DMF-d7; DEPT-135 proton coupled): 156.96; 126.10.

<Figure 2 near here>

The above characterisation was integrated with vibrational spectroscopy. Raman spectra of solid TpymT and of the synthesized complex were recorded, confirming the nature of the desired complex on the basis of the detection of a band at 341 cm^{-1}, which can be assigned to a Pt-Cl stretching mode by comparison with literature spectra. Accordingly, the derived raw formula is $[Pt_3(TPymT)(Cl)_3]^{3+} \cdot 3OH^-$ (see Supplementary Information for ^1H NMR spectra in D_2O, Raman spectra and details on Raman assignments).

3.2 Solution Behaviour

The solution behaviour of both L and Pt_3L^{3+} under physiological-like conditions was investigated spectroscopically. A substantial stability in the buffer and upon light irradiation could be assessed as the respective UV-vis signatures and fluorescence emissions did not change noticeably within hours in PB buffer as well as in NaCac buffer (see Supporting Information). The ligand alone exhibits a maximum absorption at 249 nm, while the Pt(II) complex band shifts at the lowest limits of the acceptable window with a maximum at ca. 208 nm (Figure 3, $\varepsilon_{249} = 3.79\times10^4\ M^{-1}\ cm^{-1}$ and $\varepsilon_{208} \approx 5.2\times10^5\ M^{-1}\ cm^{-1}$ respectively). The direct proportionality between absorbance and concentration of the species is obeyed (in the explored range, i.e. below ca. 3×10^{-5}M – not shown), suggesting the absence of auto-aggregation phenomena.

< Figure 3 near here>

3.3 DNA Interactions

Afterward, the interactions with DNA of the Pt_3L^{3+} complex and of the free ligand were comparatively analysed through a variety of methods to establish the strength of the occurring interactions and elucidate their nature.

3.3.1 Ethidium bromide displacement tests

The absence of any significant UV-vis signal in a window out of that of the DNA, prevents direct spectrophotometric titrations (some tests confirmed the impossibility to deconvolute the contributions of the singles species in L/DNA or Pt_3L^{3+}/DNA spectrophotometric titrations). Therefore, an ethidium bromide (EB) fluorescent intercalator displacement assay [13, 14] was used to characterise the interactions with DNA. EB is known to be essentially non-fluorescent in buffer but highly emissive when intercalated into DNA (λ^{max}_{exc} = 520 nm, λ^{max}_{em} = 595 nm). Thus, DNA was first saturated with EB until maximum fluorescence was reached, then increasing amounts of the drug (L or Pt_3L^{3+} - both non-fluorescent at λ_{exc} = 520 nm) were added to the mixture. Figure 4 shows the results obtained as F% = 100×F/F° (where F° is the read at zero addition and F is corrected for dilution effects) as a function of r = C_D/C_{DNA}.

< Figure 4 near here>

We observed that L is not able to produce significant changes in the fluorescence emission of EB/DNA, whereas Pt_3L^{3+} addition causes a nearly complete fluorescence loss already at r = C_D/C_{DNA} = ca. 4. This fluorescence decrease can be explained on the basis of an interaction of the Pt_3L^{3+} complex with DNA resulting into EB displacement from the polynucleotide base pairs.

The exchange process can be expressed by the simplified model shown as reaction (1) [15].

$$PEB + D \overset{K_{ex}}{\rightleftarrows} PD + EB \qquad (1)$$

where PEB is the EB/DNA adduct, D is the free Pt_3L^{3+} complex, PD is the Pt_3L^{3+}/DNA adduct and EB is free ethidium. It should be noted that, under the applied experimental conditions (i.e. NaCl 0.1 M/NaCac 0.01 M, pH 7.0, 25° C), the binding constant for the formation of the EB/DNA complex is relatively high (K_{EB} = 2.6×10^5 M^{-1}) [16]. The experimental results indicated that the exchange reaction is disfavoured in the case of L (too low K_{ex} value). On the other hand, K_{ex} can be calculated in the case of Pt_3L^{3+} according to equation (2) (for its derivation, see Supporting Information)

$$\frac{(C_{EB}\text{-}\,[PEB])^2}{[PEB]} = K_{ex}(C_D - C_{EB} + [PEB]) \qquad (2)$$

where C_D and C_{EB} are the total analytical complex and ethidium concentrations respectively, whereas [PEB] is calculated as $C°_{EB}\times F/F°$ (being PEB the only fluorescent species). It turns out (Figure 4 inset) that $K_{ex} = 0.11 \pm 0.2$ (total error over the triplicates). On this basis, the equilibrium constant for Pt_3L^{3+} binding to DNA would be $K = K_{ex} \times K_{EB} \approx 3\times10^4$ M^{-1}. Note that this value should be intended as indicative, as based on a simplified model that considers a 1:1 stoichiometry for the exchange process.

3.3.2 Melting tests

Afterward, DNA melting tests were performed by measuring the absorbance changes of L/DNA or Pt_3L^{3+}/DNA mixtures at 260 nm [17] Figure 5A-B shows the results as $\%A = 100\times(A\text{-}A°)/(A^{\infty}\text{-}A°)$ where A° is the absorbance plateau at low temperatures and A^{∞} is the absorbance plateau at high temperatures. Melting temperatures (T_m) are calculated as the inflection point of the sigmoid that fits the experimental data (Figure 5C – overall error on the replicates). Pt_3L^{3+} shows the strongest effects, with a destabilisation of the polynucleotide double helix that brings about a T_m decrease of about 4° C.

< Figure 5 near here>

Melting temperature changes are not a direct measure of affinity but their extent allows to comment on the ability of the binding molecule to alter the stability of the double strand. In the case of intercalation of a small planar molecule between the base pairs a major stabilisation effect is observed (usually $\Delta Tm>10°$ C, [18]), whereas destabilisation can be related to groove binding) [19].

3.3.3 Viscometry

Viscometric measurements were also carried out on both L/DNA and Pt_3L^{3+}/DNA mixtures at different reactants ratios (r = 0.25, 0.50, 0.75, 1.0, 2.0). Efflux times are treated to get the relative viscosity as $\eta/\eta° = (t - t_{solv})/(t_{DNA} - t_{solv})$ where t_{solv} and t_{DNA} are the efflux times of buffer and DNA alone, respectively. Note that, as the ligand is insoluble in the buffer and should be solved in DMSO, small amounts of the latter solvent were present in the mixtures. As this can have a non-negligible effect on the efflux times, care was taken to keep the DMSO content constant (0.4 % v/v) in all L/DNA and Pt_3L^{3+}/DNA measurements. The cubic root of $\eta/\eta°$ can be assumed as an evaluation of the elongation of the DNA strand; Figure 6 shows the results. Despite the relatively large errors inherent to the procedure, it can be clearly observed that both species do interact with DNA causing a compaction of the helix and that Pt_3L^{3+} produces the strongest effects (ca. 20% compaction for Pt_3L^{3+}/DNA respect to 8% for L/DNA). This behaviour is in contrast with intercalation [20,21] and suggests bending of DNA driven by external binding [22,23].

< Figure 6 near here>

Note that, in the case of the L/DNA system, the point at r = 2.0 seems to be slightly out of the trend, as confirmed by inspection of Figure 5C where the melting

temperature for r = 1.0 also suggests an upward trend. These data suggest some change in the binding effects in the presence of ligand excess, likely related to π–π dye-dye interactions on the DNA surface.

3.3.4 Interaction with model oligonucleotide (ESI-MS)

To shed further light on the occurring interactions we performed ESI-MS experiments after incubation of the study complex with a simple model of single strand DNA i.e. the dodecameric GG rich oligonucleotide CTACGGTTTCAC (ODN), according to the protocol developed in our laboratory [24-29]. In principle, by this approach, it is possible to describe the reaction pattern leading to metallodrug binding to the biomolecular model. Upon incubation of the study complex with the oligonucleotide at different complex to oligonucleotide ratios (i.e. 0.2:1 and 0.5:1), Pt_3L^{3+} interacts with the model oligonucleotide only for the higher concentration of complex whereas no adduct formation was observed in the case of the lower concentration. The metalation process mainly occurs through preferential coordination of small hydroxylated monoplatinum fragments to ODN after Pt_3L^{3+} complex disassembly and loss of the TPymT ligand, this representing the likely binding mechanism (see the ESI-MS spectrum in the Supplementary Information). The strong interaction occurring between platinum ions and purine nucleobases (given the known affinity of platinum drugs for N7 nitrogen of guanines [30]) might be the basis for the non-intercalative mode of binding of Pt_3L^{3+}. Moreover, the general geometry of this Pt complex is such that it can accommodate in the DNA grooves and achieve efficient interactions from the groove's size. Also, the planar geometry of Pt_3L^{3+} can drive some dye-dye π–π interactions on the DNA surface that would stabilise external binding. This effect has been already observed in the case of aromatic/hydrophobic dyes [31-33].

3.3.5 Cellular effects

Next, the antiproliferative properties of the Pt_3L^{3+} complex were measured *in vitro* against two cancer cell lines, HCT116 (colorectal, CRC) and MDA-MB-231 (breast). Pt_3L^{3+} manifested IC_{50} values of 136.5±5.2 µM and 93.2±13.4 µM in HCT116 and MDA-MB-231 respectively; in both cases this value is significantly higher than that of cisplatin, having this latter an IC_{50} of about 25 µM for these two cell lines [34,35].

4. CONCLUSIONS

In this study we have prepared and characterized, for the first time, the triplatinum complex of the TPymT ligand. The resulting complex is highly symmetric as clearly documented by the ^{1}H NMR spectra. Notably, both the free ligand and its triplatinum complex turned out to be pretty stable under physiological-like conditions. Owing to its putative planar structure and to the presence of positive charges, we argued that Pt_3L^{3+} might interact strongly with double helix DNA through intercalation. This prompted us to investigate its interactions with various DNA models through a variety of biophysical methods. Interactions with DNA were studied in comparison to the free ligand through ethidium bromide displacement, melting and viscometry assays.

Remarkably, the triplatinum complex turned out to produce far more evident changes in the DNA structure than the free ligand. However, in contrast with expectations, our results strongly favour the occurrence of a non-intercalative binding mode. Indeed, an evident - though moderate - destabilization of the DNA double helix was observed in contrast to the usually large stabilization expected for intercalation. Also, no elongation (as it should occur for intercalation) but, instead, helix compaction was highlighted by viscometric tests. These results support the concept that the positively charged triplatinum complex interacts with the DNA molecules through external/groove binding interactions. Cellular experiments on two cell lines (HCT116 and MDA-MB-231) were also carried out to assess the cytotoxic effect. The relatively high values of IC_{50} point out that Pt_3L^{3+} is scarcely effective in these cancer cell lines again disfavouring the idea of intercalative DNA binding. By overall integration of

the obtained results, it may be hypothesised that the lack of intercalation leads to relatively poor pharmacological effects, being groove binding the main binding mode for the studied complex with double stranded DNA. This view is somehow supported by ESI-MS experiments indicating that, upon reaction with the single strand dodecameric oligonucleotide, Pt binding occurs through disassembly of the Pt_3L^{3+} complex followed by coordination of small mono metallic fragments to the oligo.

Supplementary Data

NMR spectra of starting material for ligand synthesis, NMR of TpymT and PtL^{3+}, ESI-MS spectrum of complex after incubation with oligonucleotide, Raman spectra for complex characterisation, UV-Vis for stability, derivation of equation (2).

Acknowledgments

We gratefully acknowledge Beneficentia Stiftung, ITT (Istituto Toscano Tumori), Ente Cassa Risparmio Firenze (ECR) and AIRC for founding the projects (IG-16049) and "Advanced mass spectrometry tools for cancer research: novel applications in proteomics, metabolomics and nanomedicine" (Multi-user Equipment Program 2016, Ref. code 19650). COST Action CM1105 and University of Pisa (PRA_2017_25, to C.G. and T.M.) are also acknowledged. T.M. thanks AIRC-FIRC (Fondazione Italiana per la Ricerca sul Cancro) for the 3-years Fellowship for Italy, Project Code: 18044. Authors thank Prof. Carla Bazzicalupi (University of Florence) for suggesting the studies on complexes bearing 2,4,6-Tris(2-pyrimidyl)-1,3,5-triazine ligand.

Dedication

Tiziano Marzo dedicates this paper to his mother in what would have been the year of her 70th birthday.

References

[1] F. H. Case and E. Koft, J. Am. Chem. Soc., 1959, 81, 905.

[2] E. I. Lerner, S. J. Lippard, Inorg. Chem., 1977, 16, 1537.
[3] D. A. Safin, J. M. Frost, M. Murugesu Dalton Trans., 2015, 44, 20287.
[4] D. A. Safin, A. Pialat, I. Korobkov, M. Murugesu, Chem. Eur. J., 2015, 21, 6144.
[5] S. Ray, F. R. Smith, J. N. Bridson, Q. Hong, V. J. Richardson, S. K. Mandal, Inorganica Chim. Acta, 1994, 227, 175.
[6] N. Busto N., J. Valladolid, M. Martínez-Alonso, H. J. Lozano, F. A. Jalo, B. R. Manzano, A. M. Rodríguez, M. C. Carrion, T. Biver, J. M. Leal, G. Espino, B. García B., Inorg. Chem., 2013, 52, 9962.
[7] C. Metcalfe, C. Rajput, J. A. Thomas, J. Inorg. Biochem., 2006, 100, 1314.
[8] T. Biver, F. Secco, M. R. Tinè, M. Venturini, A. Bencini, A. Bianchi, C. Giorgi J. Inorg. Biochem., 2004, 98, 1531.
[9] G. Felsenfeld, S. Z. Hirschman, J. Mol. Biol., 1965, 13, 407.
[10] M. J. Waring, J. Mol. Biol., 1965, 13, 269.
[11] M. Garcia, D. M. Bassani, J. M. Lehn, G. Baum, D. Fenske, Chem. Eur. J., 1999, 5, 1234.
[12] D. A. Safin, N. A. Tumanov, A. A. Leitch, J. L. Brusso, Y. Filinchuk, M. Murugesu, Cryst. Eng. Comm., 2015, 17, 2190.
[13] W. C. Tse, D. L. Boger, 2005. A Fluorescent Intercalator Displacement Assay for Establishing DNA Binding Selectivity and Affinity. Curr. Protoc. Nucleic Acid Chem., 20:8.5:8.5.1–8.5.11.
[14] H. Lemmerhirt, S. Behnisch, A. Bodtke, C. H. Lillig, L. Pazderova, J. Kasparkova, V. Brabec, P. J. Bednarski, J. Inorg. Biochem., 2018, 178, 94.
[15] T. Biver, F. Secco, M. R. Tinnè, M. Venturini, J. Inorg. Biochem., 2004, 33.
[16] F. J. Meyer-Almes and D. Porschke, Biochemistry, 1993, 32, 4246.
[17] G. E. Plum, 2001. Optical Methods. Curr. Protoc. Nucleic Acid Chem., 00:7.3:7.3.1–7.3.17.
[18] S. Alnabulsi, E. Santina, I. Russo, B. Hussein, M. Kadirvel, A. Chadwick, E. V. Bichenkova, R. A. Bryce, K. Nolan, C. Demonacos, I. J. Stratford, S. Freeman, Eur. J. Med. Chem., 2016, 111, 33.

[19] R. Anwer, N. Ahmad, K. I. Al Qumaizi, O. A. Al Khamees, W. M. Al Shaqha, T. Fatma, J. Mol. Recognit., 2017, doi: 10.1002/jmr.2599

[20] P.C. Dedon, 2001. Determination of Binding Mode: Intercalation. Curr. Protoc. Nucleic Acid Chem. 00:8.1:8.1.1–8.1.13.

[21] I. Haq, P. Lincoln, D. Suh, B. Norden, B. Z. Chowdhry, J. B. Chaires, J. Am. Chem. Soc., 1995, 117, 4788.

[22] D. Gopalakrishnan, M. Ganeshpandian, R. Loganathan, N. S. P. Bhuvanesh, X. J. Sabinad and J. Karthikeyan, RSC Adv., 2017,7, 37706.

[23] S. B. Singh, A. S. Kumbhar , A. Khan., Chem. Eur. J., 2016, 22, 15760.

[24] T. Marzo, D. Cirri, C. Gabbiani, T. Gamberi, F. Magherini, A. Pratesi, A. Guerri, T. Biver, F. Binacchi, M. Stefanini, A. Arcangeli, L. Messori, ACS Med. Chem. Lett., 2017, 8, 997.

[25] T. Marzo, A. Pratesi, D. Cirri, S. Pillozzi, G. Petroni, A. Guerri, A. Arcangeli, L. Messori, C. Gabbiani, 2017, Inorg. Chim. Acta, 2018, 318.

[26] Y. Gothe, T. Marzo, L. Messori, N. Metzler-Nolte, Chem. Eur. J., 2016, 22, 12487.

[27] A. Pratesi, D. Cirri, M. D. Đurović, S. Pillozzi, G. Petroni, Ž. D. Bugarčić, L. Messori, Biometals, 2016, 29, 905.

[28] C. Martín-Santos, E. Michelucci, T. Marzo, L. Messori, P. Szumlas, P. J. Bednarski, R. Mas-Ballesté, C. Navarro-Ranninger, S. Cabrera, J. Alemán, J. Inorg. Biochem., 2015, 153, 339.

[29] E. Michelucci, G. Pieraccini, G. Moneti, C. Gabbiani, A. Pratesi, L. Messori, Talanta, 2017, 167, 30.

[30] S. Ahmad, 2017, Polyhedron, 138,109.

[31] R. Zhang, D. Tang, P. Lu, X. Yang, D. Liao, Y. Zhang, M. Zhang, C. Yu and V. W. W. Yam, Org. Lett., 2009, 11, 4302.

[32] T. Biver, A. Boggioni, F. Secco, E. Turriani, M. Venturini, S. Yarmoluk, Arch. Biochem. Biophys., 2007, 465, 90.

[33] T. Biver, S. Aydinoglu, D. Greco, F. Macii, Monatsh. Chem., 2018, 149, 175.

[34] S. Wang, J. Xie, J. Li, F. Liu, X. Wu, Z. Wang, Am. J. Cancer Res., 2016, 6, 1108.

[35] T. Marzo, S. Pillozzi, O. Hrabina, J. Kasparkova, V. Brabec, A. Arcangeli, G. Bartoli, M. Severi, A. Lunghi, F. Totti, C. Gabbiani, A. G. Quiroga, L. Messori, 2015, 44, Dalton Trans., 14896.

Figure Captions

Figure 1 – **a**) Chemical structures of the *tris*-2,4,6-(2-pyrimidyl)-1,3,5-triazine ligand (TPymT, L) and **b**) of its platinum complex ($[(TPymT)Pt_3(Cl)_3]^{3+}$, Pt_3L^{3+}).

Figure 2 –^{1}HNMR Spectrum of Pt_3L^{3+} recorded at 298K, DMF-d_7 (400.13 MHz): δ 9.43 (2H, d; J = 5.28 Hz); δ 8.10 (^{1}H, t; J = 5.28 Hz).

Figure 3 – Absorbance spectra of L (straight, left y-axis) and Pt3L3+ (dotted, right y-axis and inset); [NaCl] = 0.1 M, [NaCac] = 0.01 M, pH 7.0, 25.0 °C.

Figure 4. Example of EB/DNA exchange tests using L (●) or Pt_3L^{3+} (■); C_{DNA} = 1.55×10^{-4} M, $C_{EB} = 5.9\times10^{-5}$ M, r = C_D/C_{DNA}, NaCl 0.1 M/NaCac 0.01 M, pH 7.0, λ_{exc} = 520 nm, λ_{em} = 595 nm, 25.0 °C. In the inset, x = $C_D - C_{EB}$ + [EB/DNA], y = $(C_{EB}$ - $[EB/DNA])^2/[EB/DNA]$ with [EB/DNA] = $C°_{EB}\times F/F°$ and the continuous line is data fit according to equation (2).

Figure 5. Melting tests on the L/DNA (A) and Pt_3L^{3+}/DNA (B) systems at different values of r = C_D/C_{DNA}; $C_{DNA} = 2.50\times10^{-5}$ M, pH 7.0, λ = 260 nm, NaCl 0.1 M/NaCac 0.01 M. (C) Melting temperatures as a function of r for L/DNA (●) and Pt_3L^{3+}/DNA (■) systems.

Figure 6. Relative viscosity of L/DNA (●) and Pt_3L^{3+}/DNA (■) systems at different values of r = C_D/C_{DNA}; C_{DNA} = 2.0×10^{-4} M, pH 7.0, NaCl 0.1 M/NaCac 0.01 M, 25.0 °C.

Figure 1

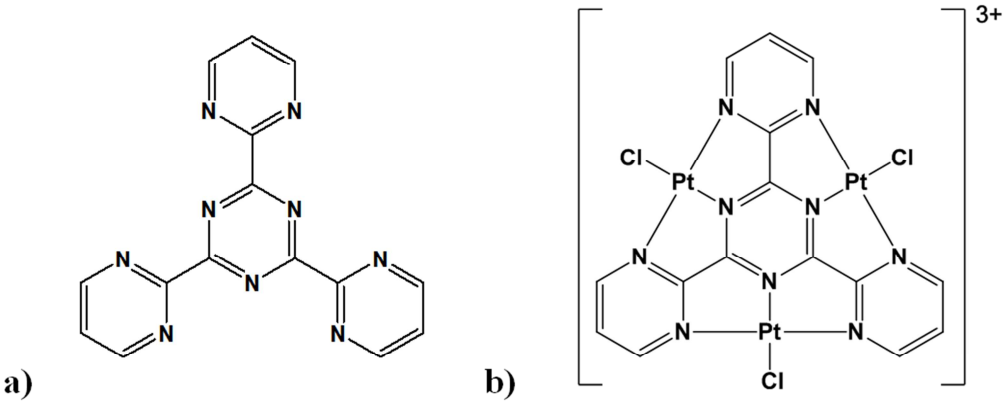

Figure 2

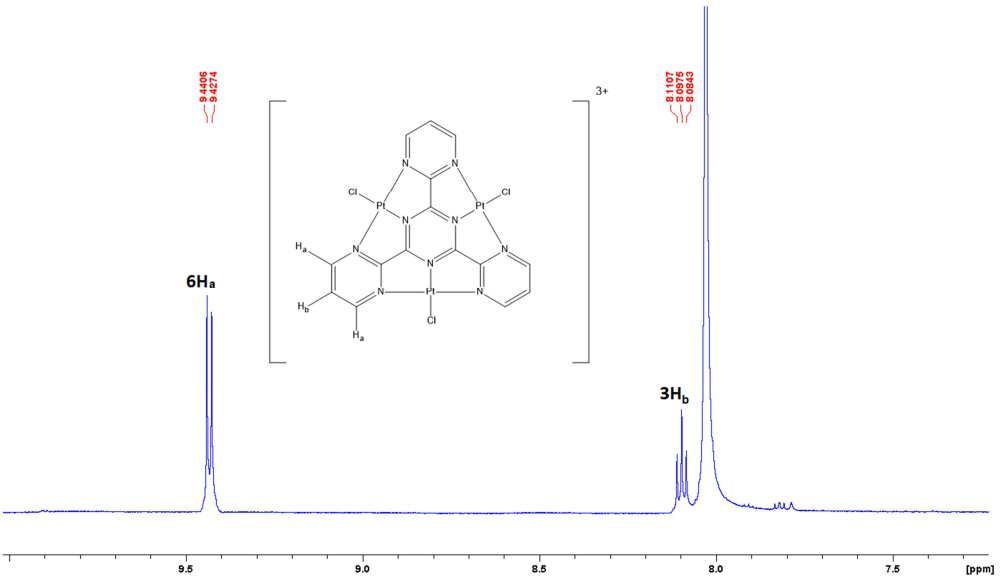

Figure 3

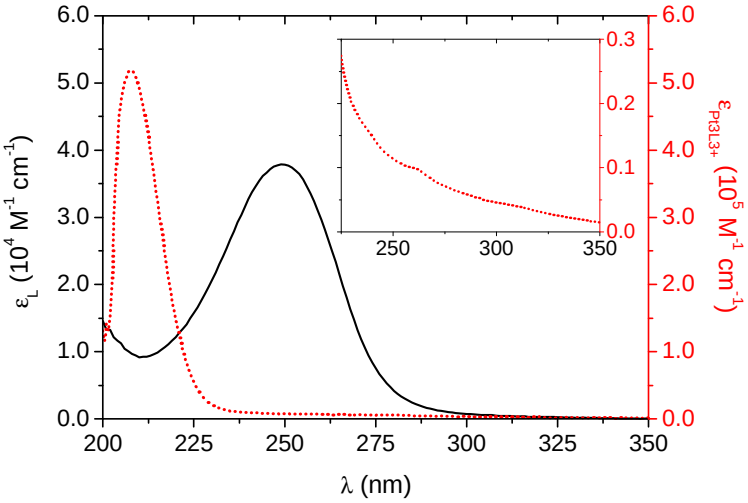

Figure 4

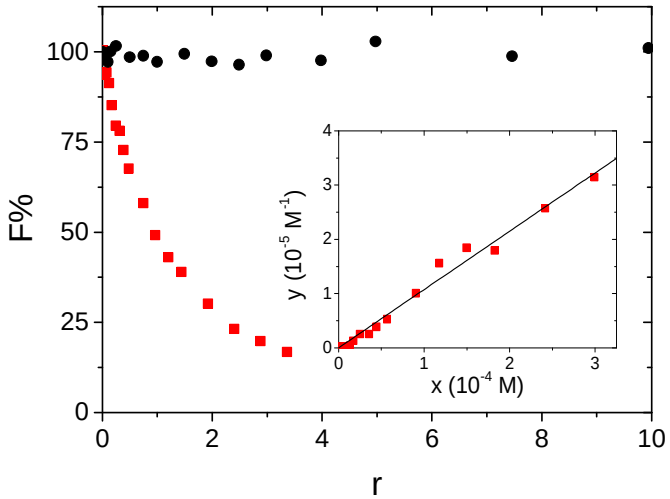

Figure 5

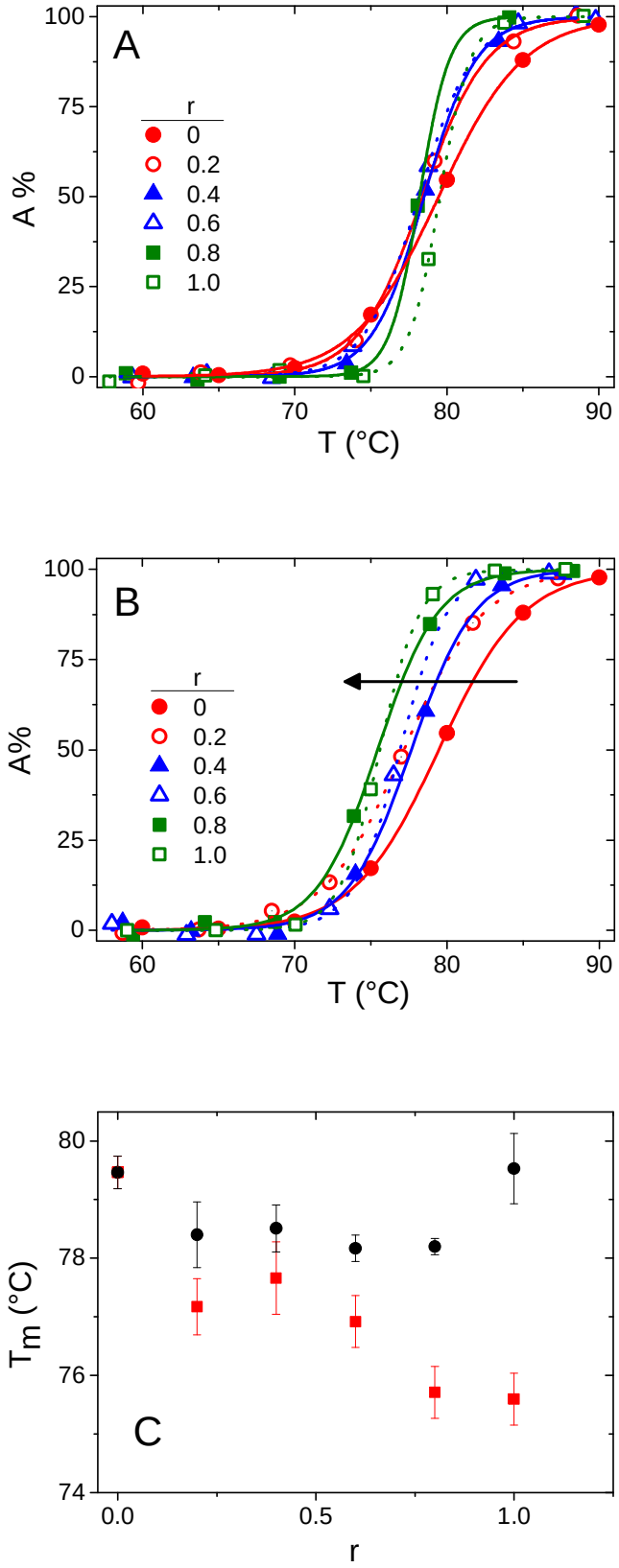

Figure 6

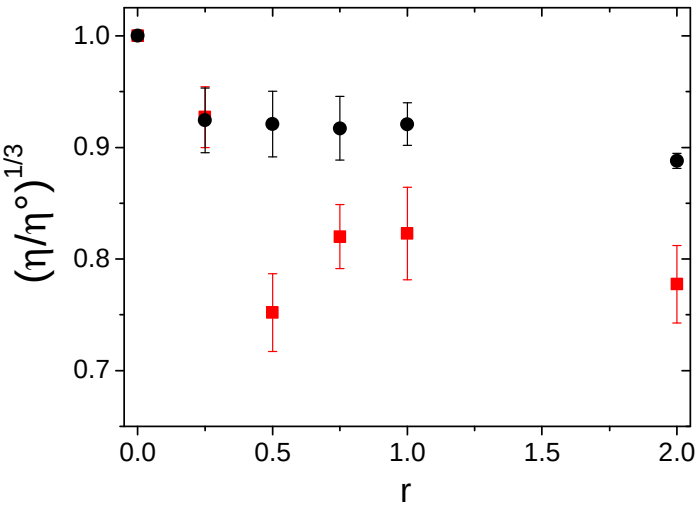
1.0
0.9
0.8
0.7
$(\eta/\eta°)^{1/3}$
0.0
0.5
1.0
1.5
2.0
r